

INTEGRATED CORROSION ASSESSMENT OF HIGH-STRENGTH GALVANIZED STEEL WIRES USING CORROSION APPEARANCE, SURFACE INFORMATION, AND FATIGUE STRENGTH

KAZUHIRO MIYACHI¹, YOUCHI SHIBUKI² AND KENSUKE SETO³

¹Tokyo Denki University
Ishizaka, Hatoyama, Hiki, Saitama, 350-0394, Japan
miyachi@g.dendai.ac.jp

² Tokyo Denki University
Ishizaka, Hatoyama, Hiki, Saitama, 350-0394, Japan
21rg040@ms.dendai.ac.jp

³ Tokyo Denki University
Ishizaka, Hatoyama, Hiki, Saitama, 350-0394, Japan
21rg044@ms.dendai.ac.jp
















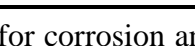

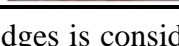
Key words: Cable-supported bridges, Corrosion, Breakage, Assessment, Maintenance, Cable corrosion, Fatigue, Rust color, S-N curve.

Abstract. *Corrosion significantly affects the fatigue performance of high-strength galvanized steel wires used in cable-supported bridges. This study quantitatively evaluated the relationship between "Corrosion Appearance," "Surface Information," and "Fatigue Strength" to understand the impact of corrosion on wire durability. Experimental results indicated that when the red rust ratio reached 27%, the fatigue strength decreased by approximately 30–33%. The presence of red rust induced crevice corrosion, leading to stress concentration and promoting fatigue crack initiation, ultimately reducing fatigue life. Additionally, corrosion led to a reduction in the wire's cross-sectional area, with an average decrease of 0.63% and a maximum decrease of 3.37%. As corrosion progressed, penetration into the steel interior increased, with corrosion depths averaging 0.11 mm and reaching a maximum of 0.21 mm. These changes contributed to further degradation in durability and fatigue resistance.*

1 INTRODUCTION

In cable-supported bridges such as suspension and cable-stayed bridges, cables are regarded as critical structural components, forming the most essential elements of the bridge structure. Bridge cables are composed of high-strength steel wires, which are typically galvanized to enhance corrosion resistance (hereinafter referred to as “wires”). However, these cables, composed of wires, are frequently exposed to harsh corrosive environments, and numerous instances of corrosion and fracture have been reported worldwide. As a result, serious consequences, including bridge collapses, have increasingly occurred. While preventive

Table 1: Comparison of wire corrosion classification schemes

Appearances of galvanized steel wire					
NCHRP guidelines		Nakamura et al.		Kinoshita et al.	
Stage	Appearance	Level	Appearance	Level	Appearance
1		Initial		Initial	
2		1		1	
3		2		2	
4		3		3	
—		—		4	
—		—		5	

maintenance for corrosion and fracture in the cables of cable-supported bridges is considered indispensable, effective strategies have not yet been fully established. Therefore, advancements in inspection and repair techniques are deemed crucial to prevent bridge collapse accidents caused by corrosion and fracture [1,2].

Study on the fatigue performance of corroded wires has been accelerated in recent years, and the effects of various corrosion levels on the S-N curve (stress range versus the number of cycles) have been quantified [3]. It is generally agreed that the fatigue life of corroded wires is significantly reduced compared to un-corroded wires, as the presence of corrosion pits is known to accelerate fatigue crack initiation and propagation, eventually leading to critical crack depths and brittle fracture. Conversely, while the qualitative relationship between corrosion appearance, surface characteristics, and fatigue strength has been recognized, limited research has been conducted to quantitatively evaluate these relationships. As a result, attention has been directed toward the quantitative evaluation of corrosion appearance and surface properties using non-contact measurement techniques such as image color analysis and 3D laser scanning. These research efforts have contributed to the development of methodologies for predicting the remaining life of corroded wires based on fracture mechanics and cellular automata [4].

Various evaluation criteria have been proposed for assessing the corrosion appearance of wires. First, the classification outlined in the NCHRP Guidelines (2004) [5] is based on field observations, where the corrosion of steel wires is visually categorized into four stages. This classification provides a general guideline applicable to various suspension bridges with parallel wire cables. Second, the classification proposed by Nakamura et al. (2013) [6] also distinguishes four levels of corrosion, presenting guidelines based on the results of accelerated corrosion tests conducted on parallel wires. Furthermore, Kinoshita et al. (2020) [7] proposed an evaluation criterion based on the rust color and the associated rust composition observed in the main cables of a suspension bridge that had been in service for over 50 years. These classification criteria are shown in Table 1. Upon comparing the three classification systems, it has been confirmed that the progression of the corrosion phenomenon appears to be largely similar. However, since all these evaluations rely on visual observation, they are likely to contain subjective elements, and their correlation with fatigue strength remains unclear.

Against this background, the establishment of reliable evaluation criteria for predicting the remaining service life of bridge cables has been strongly demanded. In this study, high-strength galvanized steel wires used in cable-supported bridges are targeted, and the correlations among "corrosion appearance," "surface characteristics," and "fatigue strength" are quantitatively evaluated.

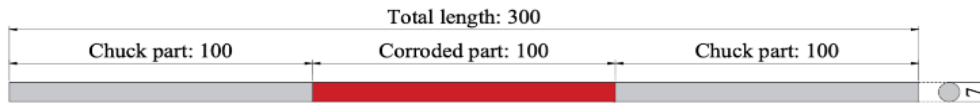


Figure 1: Dimensions of specimen (Unit: mm)

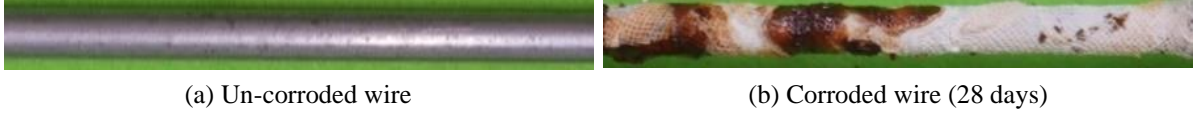


Figure 2: Appearance of specimens

2 MATERIALS AND METHODS

2.1 Specimens

The specimens used in this study were wires manufactured specifically for cable-supported bridges. The specimens had a diameter of 7 mm, a tensile strength of 1570 MPa, and a zinc coating mass of 331 g/m², equivalent to a plating thickness of approximately 50 μm, applied to the surface of the bare steel wire. These specifications are identical to those commonly used in medium- to long-span cable-supported bridges. The dimensions of the specimens are presented in Figure 1. Each specimen had a total length of 300 mm, with 100 mm allocated at both ends for fatigue test chuck sections and 100 mm in the center designated as the corroded section. The appearance of the wire prior to the accelerated corrosion test is shown in Figure 2a. For this study, 56 uncorroded wires and 38 corroded wires were employed. Here, "uncorroded wire" is defined as a wire that has not undergone any corrosion prior to the accelerated corrosion test.

To produce the corroded specimens, an accelerated corrosion test was performed under continuous moist conditions. Specifically, gauze was wrapped around the section to be corroded, immersed in a 5% saline solution for one minute, sealed in a container, and maintained at 65 °C within a constant temperature and humidity chamber [8]. This immersion process was repeated once a week for a duration of 28 days. To enable fatigue testing after the accelerated corrosion test, chuck sections were prepared at both ends of the specimens and were protected with corrosion-resistant tape to prevent corrosion. The typical appearance of the specimens after the corrosion process is shown in Figure 2b. Characteristic white rust, attributed to zinc corrosion products, and red rust, resulting from steel wire corrosion products, were observed on the surface [8].

2.2 Corrosion Appearance Analysis

After the accelerated corrosion test, the appearance of the corroded specimen was photographed using a digital camera, and the rust color distribution in the obtained image was displayed and classified using a digital image color analysis system called "Feelimage Analyzer". The analysis flow is shown in Figure 3. The photography and analysis methods were based on the techniques developed by Miyachi et al [4]. Specifically, the rust distribution ratio was quantitatively assessed using digital image color analysis software, and the corrosion level was classified based on the proportion of white rust (specific to zinc) and red rust (specific to steel). A digital single-lens reflex camera (manufactured by Canon) and a standard light source D65 specified by the International Commission on Illumination (CIE) were used for photography, with the shooting conditions designated (Figure 3a). The specimens in this study were obtained using a corrosion acceleration testing method that employed gauze wrapping,

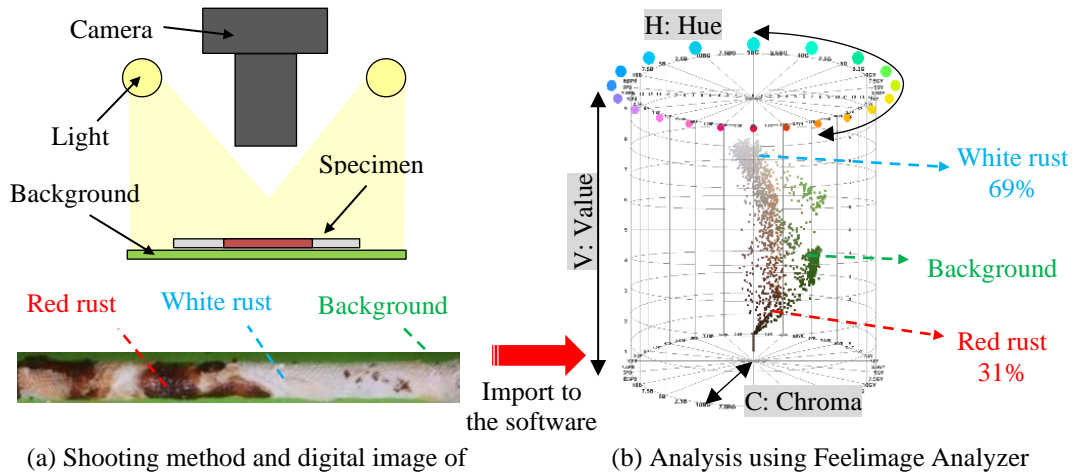


Figure 3: Analysis flow

Table 2: Setting range of Hue H, Value V, and Chroma C

Color area	H (Hue)	V (Value)	C (Chroma)
Background area	5.83Y~10.00G	0.00~10.00	0.00~14.00
Red rust area	7.00PB~3.00Y	0.00~6.00	0.00~14.00

therefore the photographs of the specimens were taken with the gauze still in place.

In this analysis system, all pixels in the image are represented using the Munsell color system (comprising hue H, value V, and chroma C) to quantitatively classify the rust color. Specifically, the rust-colored areas were distinguished from the background and each region was classified based on the designated ranges of hue, brightness, and saturation. The red rust areas were selected based on the contrast of hue H, while the remaining areas were classified as white rust (Figure 3b). Table 2 shows the color range settings for the background, red rust hue H, brightness V, and saturation C established in this study.

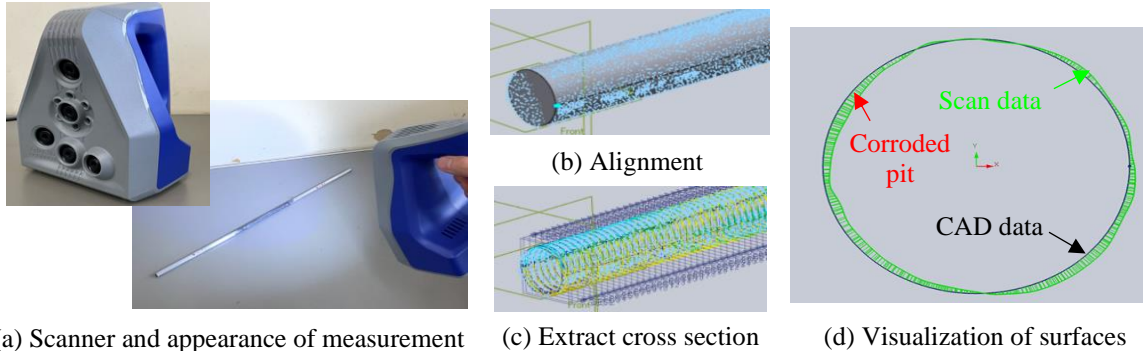
2.3 Surface Information Measurement

Subsequently, following the rust color distribution rate analysis, the surface rust was removed, and the surface roughness of the corroded wire was measured using the non-contact handheld 3D scanner Artec Spider (Artec 3D, Luxembourg), based on triangulation principles.

To remove corrosion products from the specimen surface, a polishing tool combining urethane resin and abrasives was used, ensuring that the zinc plating and base material were not damaged. Care was taken to ensure that the degree of removal remained consistent across the specimens.

The scanning process consisted of four stages: 1) equipment setup, 2) shape acquisition, 3) data processing, and 4) export. Artec Spider, with an accuracy of up to 0.05 mm, was configured with appropriate scanning conditions based on the material and shape of the object to improve the accuracy of the obtained data. The surface of each specimen was scanned, and the surface morphology of the corroded wire was analyzed, with quantitative evaluation of parameters such as surface shape, area loss, and corrosion depth. The analysis method was based on the approach proposed by Miyachi et al. [4]. The measurement flow is shown in Figure 4.

The corrosion characteristics of the specimens were determined based on existing methods [4]. Indicators for general corrosion and pitting corrosion were evaluated in terms of sectional

**Figure 4:** Measurement flow

area loss and pit depth, respectively, quantifying both local and overall characteristics (Figure 4a, 4b). The sectional area loss A_j was calculated at 1 mm intervals along the corroded length, and the maximum loss A_{\max} and average loss A_{ave} were derived (Equations (1)-(3)).

$$A_j = \left(\frac{\pi r_0^2}{\pi r_{j, \text{ave}}^2} - 1 \right) \times 100 \quad (1)$$

$$A_{\max} = \max [A_j] \text{ for all } j, j=1, 2, \dots, n \quad (2)$$

$$A_{\text{ave}} = \frac{1}{n} \sum_{j=1}^n A_j \quad (3)$$

Similarly, the maximum pit depth $d_{j, \max}$ for each section was determined, and the overall maximum d_{\max} and average d_{ave} values for each specimen were obtained (Equations (4)-(6)).

$$d_{j, \max} = \max [d_{ij}] \text{ for all } i, i=1, 2, \dots, m \quad (4)$$

$$d_{\max} = \max [d_{j, \max}] \text{ for all } j, j=1, 2, \dots, n \quad (5)$$

$$d_{\text{ave}} = \frac{1}{n} \sum_{j=1}^n d_{j, \max} \quad (6)$$

2.4 Fatigue Testing and S-N Curve selection

After the accelerated corrosion test, fatigue tests were conducted to investigate the impact of corrosion on fatigue strength. The test setup is shown in Figure 5. The fatigue tests were performed using an electromagnetic resonance fatigue testing machine (manufactured by Shimadzu Co.), and a partial single-cycle tensile fatigue test was carried out [8]. To prevent end fractures caused by stress concentration at the chucking sections during the fatigue tests, a special chucking method was employed. This method combined metal wedges designed for a diameter of $\Phi 7$ mm and MC nylon wedges at both ends of the specimens.

Un-corroded steel wires, having smooth surfaces and no defects, exhibit high fatigue strength. In the case of galvanized steel wires, the galvanizing layer serves to prevent corrosion; however, the impact of the galvanizing layer itself on fatigue properties must also be considered. While surface protection provided by the galvanizing extends fatigue life, minute defects in the plating layer may influence fatigue strength. By comprehensively evaluating these factors and adopting 2×10^6 cycles as the standard, a practical and reliable assessment is achievable. During fatigue testing, constant stress is repeatedly applied to the specimen, and the number of cycles to failure is recorded. Based on this data, an S-N curve (stress versus

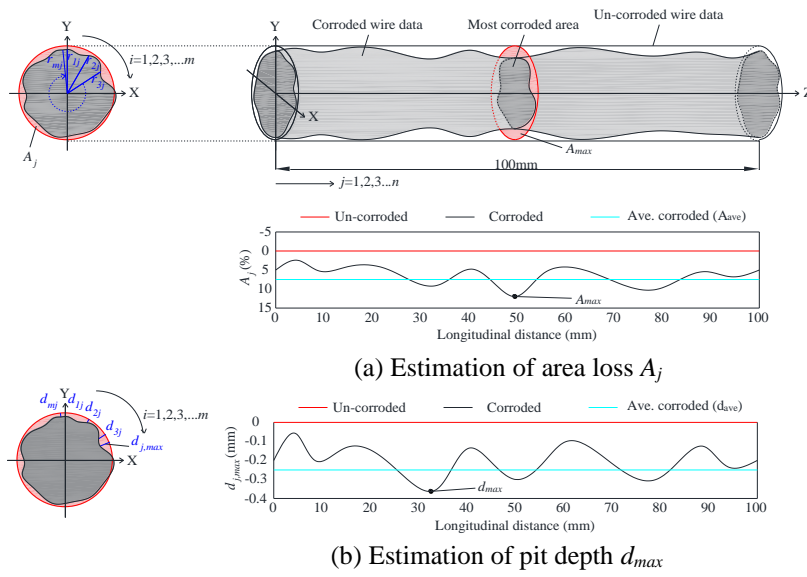


Figure 4: Method used for estimating corrosion indicators

number of cycles curve) is constructed. For these reasons, it is common practice to adopt 2×10^6 cycles as the criterion for determining the fatigue limit. For un-corroded wires, this criterion was also applied as the standard for evaluating the fatigue limit (Japanese Society of Steel Construction, 1998) [9].

Conversely, as corrosion progresses, microcracks and pits (small holes) form on the surface of the steel wires [4]. These features increase the likelihood of stress concentration and subsequently reduce fatigue strength. Un-corroded wires tested within the range below the fatigue limit can withstand infinite repeated stress. However, corroded wires tend to fail after fewer cycles, even within the same stress range, due to the progression of damage caused by corrosion, which shortens their fatigue life. In environments where wires are highly susceptible to corrosion, it becomes necessary to design wires considering the fatigue limit of corroded wires. To ensure safety, it is critical to account for the reduction in strength due to corrosion and develop appropriate maintenance and management plans.

Therefore, standard fatigue tests were conducted on un-corroded wires, and an S-N curve was constructed to evaluate the fatigue limit. Based on the fatigue test conditions from previous S-N curve studies, a minimum stress value of 500 MPa was selected as a reference [8]. The S-N curve was plotted by varying the stress amplitude, and the fatigue limit was determined.

The S-N curve, which represents the fatigue characteristics of a material by graphing the relationship between stress amplitude (S) and fatigue life (N), was selected for high-strength galvanized steel wire in this study considering the following points. When the structure involved is related to welded structures, the S-N curve provided by the International Institute of Welding (IIW) is often the most appropriate [10]. If the design standards are based on Eurocode, the S-N curve from Eurocode is typically used, as Eurocode provides a standardized approach across the European Union and is suitable for the design of civil and structural engineering projects [11]. For conservative designs or when emphasis is placed on manufacturing and environmental variations, the S-N curve from IIW is preferable. The IIW guidelines consider a wider range of data and variations, which can enhance the long-term reliability of high-strength galvanized steel wire. Therefore, in cases where high-strength

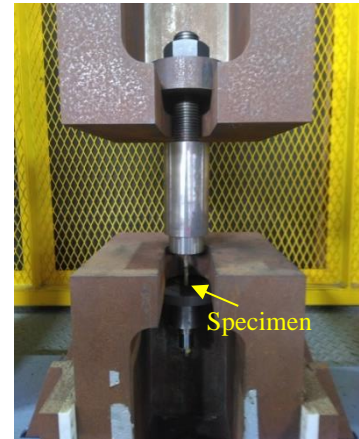


Figure 5: Fatigue test

galvanized steel wire is used under stringent conditions and a conservative design that considers variations is required, the S-N curve provided by IIW was selected.

The S-N curve is obtained by regression analysis, as per equations (7)-(10) below, following the procedure proposed by IIW (International Institute of Welding) [10]:

$$S^m N = C \Leftrightarrow \log N = \log C - m \log S \quad (7)$$

where m is the slope and $\log C$ is the intercept, and they are obtained from following equations (8) and (9).

$$\text{Slope: } m = \frac{\sum_{i=1}^n \log S_i \log N_i - \frac{1}{n} (\sum_{i=1}^n \log S_i) (\sum_{i=1}^n \log N_i)}{\sum_{i=1}^n (\log S_i)^2 - \frac{1}{n} (\sum_{i=1}^n \log S_i)^2} \quad (8)$$

$$\text{Intercept: } \log C = \frac{1}{n} \sum_{i=1}^n \log N_i + m \frac{1}{n} \sum_{i=1}^n \log S_i \quad (9)$$

For design purposes, limits or bounds must be set to bound a certain proportion of the experimental data (usually 95%). These bounds are often termed ‘prediction limits’, rather than ‘confidence limits’ to avoid confusion with the confidence limits on the coefficients of the regression line, and are given by equation (10):

$$\log N_{p\%}^{\pm} = (\log C - m \log S) \pm t \hat{\sigma} \sqrt{1 + \frac{1}{n} + \frac{(\log S - \overline{\log S})^2}{\sum_{i=1}^n (\log S_i - \overline{\log S})^2}} \quad (10)$$

where $\log C$ and m are the coefficients of the regression line through the n data points ($\log S_i, \log N_i$), $\overline{\log S}$ is the mean of the n values of $\log S_i$, t is the appropriate percentage point of Student's t distribution $t(0.05, n-2)$, with f degrees of freedom, $\hat{\sigma}$ is the best estimate of variance of the data about the regression line, which is equal to the sum of squared residuals divided by the number of degrees of freedom f , and f is equal to $n-2$ in the case where the two coefficients of the regression line have both been estimated from the data.

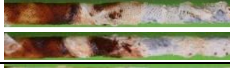
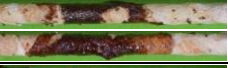







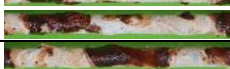


















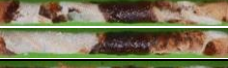






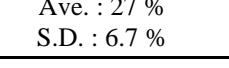
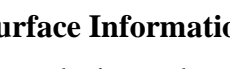

The inclusion of run-out tests has a significant influence on the estimated S-N relationships, not just at low stress range values to which these cases correspond, but also on the higher stress range values where no such cases exist. It was concluded that run-outs could be excluded from the final analysis and related comparisons, considering that the proportion of run-outs was higher in the un-corroded database compared to the corroded database [12].

3 RESULTS AND DISCUSSION

3.1 Corrosion Appearance and Its Quantification

Based on the analysis results of rust color distribution rates of test specimens, which were examined in the preceding process. The evaluation results of rust color distribution rates are shown in Table 3. The average rust color distribution rates and standard deviations for each corrosion promotion period were as follows: 28 days (38 specimens): Red rust rate $27 \pm 6.7\%$. The red rust rate for each test specimen was calculated as the average rust color distribution obtained from images of the front and back surfaces of the specimen. In this study, red rust, which is a corrosion product of base metal affecting fatigue strength, is defined as the evaluation criterion for corrosion appearance. From this point onward, $R = 27\%$ will be used to represent the above values.

Table 3: Analysis results of the rust color distribution rate of corroded wires (28 days, R=27%)

No.	Appearance	Red (%)	No.	Appearance	Red (%)	No.	Appearance	Red (%)
1		30	14		41	27		31
2		26	15		40	28		26
3		38	16		25	29		29
4		34	17		29	30		24
5		35	18		26	31		27
6		33	19		14	32		23
7		37	20		32	33		19
8		29	21		24	34		9
9		28	22		31	35		21
10		31	23		22	36		17
11		28	24		31	37		27
12		24	25		24	38		23
13		29	26		17	Ave. : 27 % S.D. : 6.7 %		

3.2 Surface Information and Its Implications

The analysis results of the surface information for the corroded wires are shown in Table 4. The average area loss rate was 0.6[%], the maximum area loss rate was 3.4[%], the average pit depth was 0.11[mm], and the maximum pit depth was 0.21[mm]. Some specimens exhibited an increase in area loss, which was due to corrosion products not being completely removed. During the early stages of white rust formation, dense and hard rust is formed, which may have made it difficult to remove completely.

The indicators derived from the surface information in this study are highly effective for evaluating corroded wires in actual field conditions. Specifically, they are expected to be useful in the following ways: Quantification of Corrosion Progression: If the wire diameter and corrosion depth can be measured, the corrosion progression can be clearly understood by comparing these values with the quantified surface information obtained above. For example, the current corrosion state can be compared with other standards based on the area loss rate and pit depth. Complementary Evaluation Method: In cases where evaluating the appearance, such as rust flaking, is difficult, the surface information can serve as a complementary tool. Particularly, since dense and hard rust is formed during the early stages of corrosion, visual evaluation alone may make it difficult to accurately assess the condition. However, by utilizing quantitative measurement data, the impact of rust can be supplemented, leading to improved

Table 4: Surface information of Corroded wires (R=27%)

No.	A _{ave} (%)	A _{max} (%)	d _{ave} (mm)	d _{max} (mm)	No.	A _{ave} (%)	A _{max} (%)	d _{ave} (mm)	d _{max} (mm)	No.	A _{ave} (%)	A _{max} (%)	d _{ave} (mm)	d _{max} (mm)
1	0.23	5.37	0.24	0.41	15	-0.07	3.20	0.09	0.18	29	0.67	4.47	0.11	0.19
2	1.61	4.25	0.13	0.18	16	-0.07	3.20	0.09	0.18	30	-0.05	1.84	0.11	0.23
3	2.25	5.82	0.14	0.25	17	1.02	2.70	0.10	0.23	31	0.48	3.36	0.10	0.21
4	1.56	4.47	0.11	0.17	18	-0.39	2.37	0.09	0.18	32	0.45	2.11	0.09	0.19
5	0.84	6.29	0.12	0.28	19	0.56	3.58	0.10	0.19	33	1.11	3.65	0.17	0.28
6	-1.00	1.04	0.07	0.13	20	-0.05	1.74	0.09	0.12	34	0.05	2.99	0.10	0.24
7	-0.24	1.28	0.10	0.18	21	0.27	2.53	0.17	0.31	35	-0.09	1.88	0.09	0.16
8	2.92	4.79	0.13	0.20	22	3.78	6.13	0.17	0.24	36	-2.00	0.71	0.07	0.14
9	1.13	2.22	0.13	0.23	23	-0.33	2.58	0.09	0.19	37	0.63	3.69	0.10	0.17
10	1.03	3.96	0.10	0.20	24	0.26	5.92	0.10	0.25	38	-1.28	1.37	0.07	0.14
11	0.80	2.60	0.17	0.26	25	0.84	5.05	0.15	0.24	Ave.	0.63	3.37	0.12	0.21
12	0.01	2.24	0.09	0.14	26	2.72	4.44	0.14	0.26	S.D.	1.14	1.52	0.04	0.06
13	0.14	1.95	0.11	0.19	27	1.00	2.86	0.15	0.25					
14	2.75	6.12	0.17	0.28	28	0.31	3.33	0.09	0.17					

evaluation accuracy. In this way, the quantified surface information can serve as a reliable indicator for making more accurate judgments in the evaluation of corroded wires in the field.

3.3 Fatigue Strength Reduction Due to Corrosion

The test results for un-corroded and corroded wires are shown in Tables 5 and 6. The relationship between the stress range S and the number of cycles N leading to fracture is summarized. All specimens fractured within the evaluation area (the central 100 mm section). The determination of the fatigue limit for un-corroded wires was considered as follows. The un-corroded wire specimens reached 2×10^6 cycles under the following conditions: Stress amplitude of 600 MPa: Achieved by 33% of the specimens. Stress amplitude of 550 MPa: Achieved by 100% of the specimens. Stress amplitude of 500 MPa: Achieved by 91% of the specimens. In this case, the fatigue limit is typically defined as the maximum stress amplitude at which all or nearly all specimens (generally 90% or more) can withstand the specified number of cycles without failure. Based on this criterion, the following results were obtained: At a stress amplitude of 600 MPa, only 33% of the specimens endured, and therefore it is not considered the fatigue limit. At a stress amplitude of 550 MPa, 100% of the specimens endured, making this a strong candidate for the fatigue limit. At a stress amplitude of 500 MPa, 91% of the specimens endured.

However, since 100% of the specimens endured at 550 MPa, 550 MPa is considered a more appropriate fatigue limit. Nonetheless, considering a more conservative approach, the fatigue limit in this case was determined to be 500 MPa.

The S - N curves for un-corroded and corroded wires, including the mean line (50%) and the conservative 'design' line (95%), are found to be as follows: in accordance with the equations (11)-(14). The S - N curves for the un-corroded and corroded wires, summarized from the following equations, are shown in Figure 6.

The mean line of S - N relationship (50%)

$$\text{Un-corroded wires} \quad S^{4.5}N=10^{17.9} \quad (11)$$

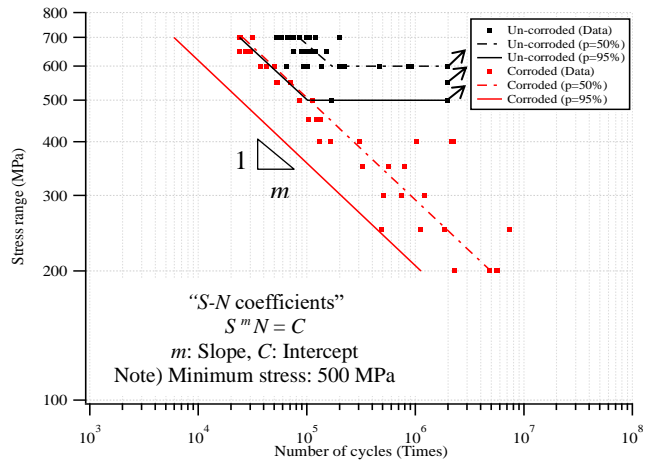
$$\text{Corroded wires (R=27\%)} \quad S^{4.2}N=10^{16.4} \quad (12)$$

Table 5: Test results of un-corroded wires

No.	S (MPa)	N (Times)	No.	S (MPa)	N (Times)
1	700	66000	29	600	223000
2	700	85000	30	600	136000
3	700	59000	31	600	93000
4	700	75000	32	600	2000000
5	700	68000	33	600	2000000
6	700	99000	34	600	2000000
7	700	202000	35	600	2000000
8	700	121000	36	550	2000000
9	700	72000	37	550	2000000
10	700	71188	38	550	2000000
11	700	69509	39	550	2000000
12	700	52938	40	550	2000000
13	700	106237	41	550	2000000
14	700	86650	42	550	2000000
15	650	75000	43	550	2000000
16	650	120000	44	550	2000000
17	650	94000	45	550	2000000
18	650	90000	46	500	170000
19	650	112000	47	500	2000000
20	650	151000	48	500	2000000
21	650	104000	49	500	2000000
22	650	76000	50	500	2000000
23	600	102000	51	500	2000000
24	600	65000	52	500	2000000
25	600	472000	53	500	2000000
26	600	869000	54	500	2000000
27	600	924000	55	500	2000000
28	600	199000	56	500	2000000

Table 6: Test results of corroded wires (R=27%)

No.	S (MPa)	N (Times)	No.	S (MPa)	N (Times)
27	700	24,247	19	400	2,243,892
26	700	23,780	17	400	305,530
28	700	31,730	13	400	165,142
29	650	23,935	16	400	1,027,552
30	650	27,264	3	400	130,372
31	650	30,163	14	350	326,860
32	600	42,098	15	350	562,762
33	600	37,826	12	350	789,001
34	600	50,404	21	300	1,224,435
35	550	54,142	11	300	752,655
36	550	52,006	10	300	510,660
37	550	71,440	9	250	7,365,368
38	500	112,395	4	250	1,127,336
25	500	84,773	8	250	1,847,773
24	500	86,182	7	250	493,252
23	450	103,385	6	200	2,299,850
22	450	133,987	5	200	5,632,875
18	450	122,139	1	200	4,860,027
20	400	2,135,712	2	200	4,786,886

**Figure 6:** *S-N* curve of un-corroded and corroded wires

The design line of *S-N* relationship (95%)



$$\text{Un-corroded wires} \quad S^{4.3}N=10^{16.6} \quad (13)$$

$$\text{Corroded wires (R=27\%)} \quad S^{4.2}N=10^{15.7} \quad (14)$$

The corrosion wires with R=27% caused the slope *m* to decrease slightly, from 4.3 to 4.2, respectively. This corresponds to a reduction of approximately 2.3% for R=27%. These changes, though small, indicate a quantifiable decrease in fatigue strength and could have significant implications for long-term fatigue performance.

Furthermore, the intercept *C* decreased from $10^{16.6}$ to $10^{15.7}$, representing reductions of about 0.9%, respectively. These decreases highlight the quantitative impact of corrosion on fatigue life and serve as critical indicators for evaluating its effects.

Table 7: Evaluation criteria derived from the corrosion appearance and fatigue strength

Condition of wires “Appearances”	Corrosion appearance “Red rust rate”	Surface information Area loss & Pit depth	Reduction rate of Fatigue strength & <i>S-N</i> Curve formula
	0 %	-	0% (mean): $S^{4.5}N=10^{17.9}$ 0% (design): $S^{4.3}N=10^{16.6}$
	27 ± 6.7 %	$A_{ave}: 0.63 \pm 1.14$ % $A_{max}: 3.37 \pm 1.52$ % $d_{ave}: 0.12 \pm 0.04$ mm $d_{max}: 0.21 \pm 0.06$ mm	33% (mean): $S^{4.2}N=10^{16.4}$ 30% (design): $S^{4.2}N=10^{15.7}$

The reduction rate of fatigue strength was calculated using equation (15) as follows:

$$Reduction\ rate = \frac{Stress\ of\ uncorroded\ specimen - Stress\ of\ corroded\ specimen}{Stress\ of\ uncorroded\ specimen} \times 100 \quad (15)$$

Mean line: Fatigue strength decreases by approximately **33%**

Design line: Fatigue strength decreases by approximately **30%**

Therefore, it has been clarified that the fatigue strength of the corroded wire with $R = 27\%$ obtained in this study is approximately 30% lower compared to the un-corroded wire.

3.4 Integrated Assessment of Corrosion

The quantitative results related to the corrosion appearance, surface information, and fatigue strength of the wires are integrated and shown in Table 7. Previous corrosion evaluation criteria for wires, as shown in Table 1, only provided descriptions of corrosion levels and appearances linked to corrosion appearance. However, in this study, attention was given to the rust color (red rust) of the base material steel, which is responsible for the strength in the corrosion level criteria. The color of the red rust obtained from the corrosion appearance was quantified and standardized, considering surface information and fatigue strength related to the corrosion appearance. Specifically, when the red rust ratio in the corrosion appearance reaches 27%, the average area reduction rate of the surface information tends to be 0.6%, and the average pit depth is 0.11 mm. Additionally, regarding fatigue strength, it decreases by approximately 30% compared to un-corroded wires.

4 CONCLUSIONS

In this study, the effect of corrosion on the fatigue strength of high-strength galvanized steel wires used in cable-supported bridges was evaluated, and the potential correlation among "Corrosion Appearance," "Surface Information," and "Fatigue Strength" was quantitatively demonstrated.

- The results showed that when the red rust ratio reached 27%, the fatigue strength decreased by approximately 30–33%. The presence of red rust was found to induce crevice corrosion on the steel surface, leading to stress concentration and promoting fatigue crack initiation, thereby reducing fatigue life.
- Additionally, a reduction in the cross-sectional area due to red rust was observed, with an average decrease of 0.63% and a maximum decrease of 3.37%. This reduction in cross-sectional area directly affected tensile and fatigue strength, and as red rust progressed, an increase in corrosion depth and penetration of corrosion into the steel interior were noted. The corrosion depth was measured to be an average of 0.11 mm

and a maximum of 0.21 mm, and this increase led to a decline in durability and a further reduction in fatigue life.

The findings of this study hold significant implications for practical applications and future bridge maintenance strategies. By quantifying the effects of corrosion appearance on fatigue strength, a more objective and reliable method for assessing the condition of galvanized steel wires used in bridges can be provided, contributing to enhanced safety and more targeted maintenance efforts. Future research should focus on investigating fatigue strength behavior under high red rust ratios exceeding 50% and conducting a detailed analysis of the long-term degradation process in corrosive environments.

ACKNOWLEDGEMENTS

In this study, the authors would like to acknowledge the support of the JSPC KAKENHI JP [grant number 23K13397].

REFERENCES

- [1] Colford, B. R., Forth Road Bridge - maintenance and remedial works, *Proceedings of the Institution of Civil Engineers, Bridge Engineering* 161, 2008; 125-132.
- [2] Nakamura S. and Miyachi K., Ultimate Strength and Chain-Reaction Failure of Hangers in Tied-Arch Bridges, *Structural Engineering International*, Vol 31, 2020; pp. 136-146.
- [3] Li H, Lan CM, Ju Y, Li DS. Experimental and numerical study of the fatigue properties of corroded parallel wire cables. *Journal of Bridge Engineering. ASCE.* 17 (2); 2012. 211–220.
- [4] Miyachi K, Chryssanthopoulos MK, Nakamura S. Experimental assessment of the fatigue strength of corroded bridge wires using non-contact mapping techniques. *Corrosion Science.* Vol.178; 2021. Available from: DOI: 10.1016/j.corsci.2020.109047.
- [5] NCHRP Report 534. Guidelines for Inspection and Strength Evaluation of Suspension Bridge Parallel Wire Cable; 2004. 17-25.
- [6] Nakamura S, Suzumura K. Experimental Study on Fatigue Strength of Corroded Bridge Wires. *Journal of Bridge Engineering. ASCE.* 18(3); 2013. 200-209.
- [7] Kinoshita K, Yano Y, Hatasa Y, Hasuike R, Miyachi K. Examination of corrosion evaluation criteria based on rust composition analysis in corrosion investigation of actual suspension bridge main cables. *Journal of Structural Engineering.* 66A; 2020. 431-442.
- [8] Miyachi K., Masumi T. and Shimada S., Structural transformation and aesthetic design of cable-stayed bridges introducing arch ribs, *Risk-Based Strategies for Bridge Maintenance, proceedings of New York City Bridge Conference 2023*, 2023; 55-66.
- [9] Japanese Society of Steel Construction. Guidelines of Fatigue Design of Steel Structures. Gihodo; 1998.
- [10] Schneider CRA, Maddox SJ. Best Practice Guide on Statistical Analysis of Fatigue Data. International Institute of Welding TWI Statistics Report; 2003. 1–20.
- [11] Eurocode 3: Design of steel structures - Part 1-9: Fatigue, EN; 1993.
- [12] Sarkani S, Mazzuchi TA, Lewandowski D, Kihl DP, Runout analysis in fatigue investigation. *Engineering Fracture Mechanics.* 74; 2007. 2971–2980.